INSTITUTE OF PHYSICS PUBLISHING SUPERCONDUCTOR SCIENCE AND TECHNOLOGY

Supercond. Sci. Technol. **17** (2004) S213–S216 PII: S0953-2048(04)73327-8

Development and study of Rutherford-type cables for high-field accelerator magnets at Fermilab

E Barzi, N Andreev, C Boffo, E Borissov, L Elementi, L Del Frate, R Yamada and A V Zlobin

Fermi National Accelerator Laboratory, Batavia, IL 60510, USA

Received 19 November 2003
Published 19 March 2004
Online at stacks.iop.org/SUST/17/S213 (DOI: 10.1088/0953-2048/17/5/024)

Abstract
Fermilab is developing a new generation of high-field superconducting magnets for future accelerators based on Nb_3Sn. Rutherford-type cables of 27 and 28 strands of various structures, packing factors, with and without a stainless steel core, were fabricated at Fermilab out of Cu, NbTi and various Nb_3Sn strands. The effect of cabling degradation was measured. A method was developed to simulate cabling and possibly understand the strains applied during the process. This paper summarizes the results of such R&D efforts at Fermilab.

(Some figures in this article are in colour only in the electronic version)

1. Introduction

Within the High Field Magnet (HFM) project at Fermilab, Nb_3Sn dipole magnets are being developed and studied [1, 2]. Cost-effective accelerator magnets require high critical current density in the non-Cu section of the strand, ideally about 3000 A mm^{-2} at 4.2 K and 12 T. The need for heat-treating the Nb/Sn composite to form brittle Nb_3Sn imposes a completely different technology in magnet fabrication with respect to NbTi. Typically the coil has to be first wound and then reacted as a whole. During this process, many factors can lead to reduction of the critical current, I_c, of the original strand. Among the factors that reduce I_c are strand plastic deformation during cabling (before reaction), Sn leaks (during reaction), and cable compression in the coil (after reaction) during magnet assembly and operation. This latter factor is due to J_c sensitivity of Nb_3Sn to strain. This paper will focus on the study of the cabling effect, whereas reference is made to [3] for measurements of the transverse pressure effect.

Fermilab's cable R&D programme encompasses extensive studies of Rutherford-type cables of various designs and technologies. Using a compact cabling machine with up to 28-strand capacity, 1 mm strand cables with aspect ratios of about 8, packing factors from 85 to 95%, with and without a stainless steel core, were fabricated at Fermilab out of Cu, NbTi and modified jelly roll (MJR), powder-in-tube (PIT) and internal tin (IT) Nb_3Sn strands [4]. A method was developed to simulate cabling and possibly understand the strains applied during the process. As accelerator magnets also demand excellent field quality, two-stage cables, where the 1 mm strand was made of an assembly of seven smaller sub-strands (see figure 1, bottom), were also studied as a way of reducing the effective filament diameter.

2. Nb_3Sn strands and cables

Several kilometres of multifilamentary Nb_3Sn strands produced using the MJR, IT (low-tin ITER type) and PIT technologies were or are in the process of being purchased by Fermilab from Oxford Superconducting Technology (OST), Outokumpu (former Intermagnetics General Corporation (IGC)) and ShapeMetal Innovation (SMI), respectively. These strand parameters are shown in table 1.

One-stage and two-stage 28-strand cables with rectangular and keystone cross-sections, and various packing factors, were fabricated in-house with and without a 9.525 mm × 0.025 mm core made of 316-L annealed stainless steel. Some cross-sections are shown in figure 1. Typical variations of nominal cable width and thickness along the cable length during cable fabrication are plotted in figure 2.

The cable packing factor (PF) is one of the parameters which determines the level of strand mechanical deformation

Table 1. Strand parameters.

Strand parameter	MJR	IT (ITER)	PIT
Strand diameter (mm)	1.000 ± 0.001	1.000 ± 0.001	1.000 ± 0.001
J_c (12 T) (A mm^{-2})	~2000	~650	~1700
I_c (12 T) (A)	~800	~200	~700
d_{eff} (μm)	<110	<5	<50
Cu (%)	47 ± 0.3	58.7 ± 0.3	48.7 ± 0.3
RRR	30–180	>300	>150
Twist pitch (mm/turn)	25 ± 10	13 ± 3	20 ± 3

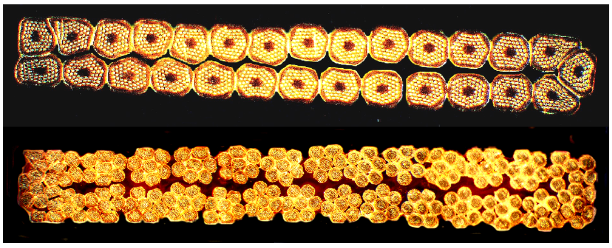

Figure 1. Cross-sections of 28-strand cables: one-stage cable (top); two-stage cable (bottom).

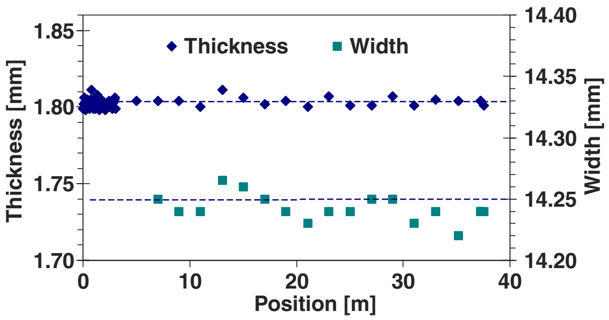

Figure 2. Typical variations of cable width and thickness along the length of a keystoned cable: width $= 14.243 \pm 0.011$ mm, thickness $= 1.802 \pm 0.003$ mm.

during cable fabrication. It is defined as follows:

$$\mathrm{PF} = \frac{n\pi d^2}{4(wt - A_{\mathrm{Core}})\cos\psi},$$

where n is the number of strands in the cable, d is the strand diameter, w and t are the average width and thickness, Ψ is the lay angle and A_{Core} the core cross-section. Samples with different packing factors were obtained by varying cable mean thickness, whereas cable width, lay angle and the keystone angle, α were kept within 14.24 ± 0.025 mm, $14.5° \pm 0.1°$ and $0.9° \pm 0.1°$, respectively. For rectangular cables, α was $0.0° \pm 0.1°$. Tables 2–4 show the one-stage cable parameters (under 'type', 'R' stands for rectangular and 'KS' for keystoned geometry), whereas the two-stage cable geometry is specified in table 5.

3. Sample preparation and measurement procedure

Virgin (round) strands and strands extracted from each cable were heat treated in argon atmosphere according to the schedules in table 6. Voltage–current (VI) characteristics were measured in boiling He at 4.2 K, in a transverse magnetic field, B, as described in [4]. The estimated uncertainty of the I_c measurements in this study is within ±1% at 4.2 K and 12 T.

Table 2. PIT cable parameters.

PIT2	Core	Type	Thickness (mm)	PF (%)
1	Y	R	1.950	84.9
2	Y	KS	1.880	85.6
3	Y	KS	1.860	86.6
4	Y	KS	1.800	89.5
5	Y	KS	1.760	91.5
6	N	R	1.970	83.6
7	N	KS	1.874	85.1
8	N	KS	1.843	86.6
9	N	KS	1.801	88.6
10	N	KS	1.720	93.0

Table 3. MJR cable parameters.

MJR	Core	Type	Thickness (mm)	PF (%)
1	Y	R	1.950	84.9
2	Y	KS	1.880	85.6
3	Y	KS	1.860	86.6
4	Y	KS	1.800	89.5
5	Y	KS	1.775	90.7

Table 4. IT (ITER) one-stage cable parameters.

ITER	Core	Type	Thickness (mm)	PF (%)
1	N	R	1.970	83.6
2	N	KS	1.820	88.7
3	N	KS	1.760	90.7
4	N	KS	1.722	92.8
5	Y	R	1.970	84.3
6	Y	KS	1.882	86.3
7	Y	KS	1.841	87.9
8	Y	KS	1.804	89.1
9	Y	KS	1.762	91.2

Table 5. Two-stage ITER cable parameters.

Core	Type	Thickness (mm)	PF[a] (%)
N	R	1.970	83.6
N	KS	1.854	86
N	KS	1.833	87
N	KS	1.761	90.6
N	KS	1.721	92.7

[a] Does not include compaction of the 1 mm strand assembly.

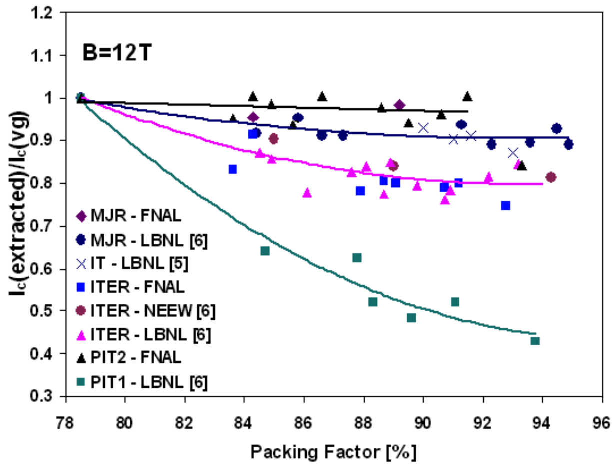

Figure 3. Normalized I_c at 4.2 K and 12 T as a function of the packing factor for the extracted IT, MJR and PIT Nb_3Sn strands.

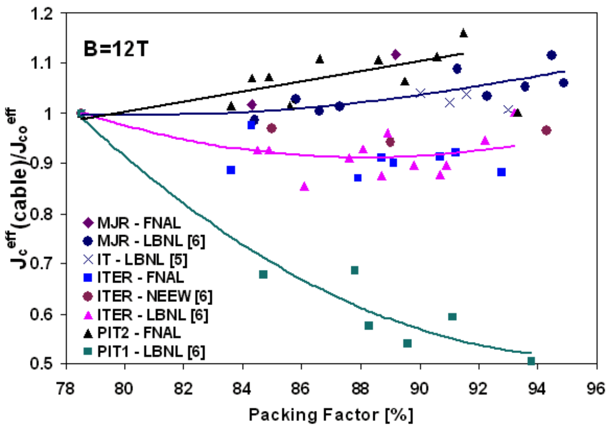

Figure 4. Effective cable J_c at 4.2 K and 12 T as a function of the packing factor.

Table 6. Heat treatment schedules.

Cable		Heat treatment	Step 1	Step 2
ITER, MJR	FNAL	Ramp rate (°C h^{-1})	30	6
		Temperature (°C)	200	700
		Duration (h)	0	40
PIT2	SMI	Ramp rate (°C h^{-1})	25	
		Temperature (°C)	655	
		Duration (h)	170	

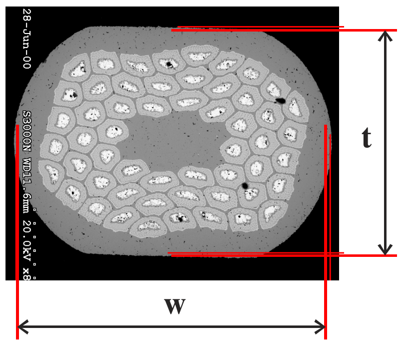

Figure 5. Cross-section of the rolled strand.

4. Test results and discussion

4.1. I_c degradation due to cabling

The results of I_c measurements made on round virgin strands were compared with those made on strands extracted from the fabricated cables. The I_c degradation at 4.2 K and 12 T, expressed as the I_c of an extracted strand normalized to the I_c of the virgin strand, is shown in figure 3 as a function of PF. The effective cable critical current density, J_c^{eff}, at 4.2 K and 12 T, normalized to the effective J_c of a cable made of undeformed round strands (theoretical PF of 78.5%), is plotted in figure 4 as a function of PF. Both plots also show a comparison with results obtained from previous studies [5, 6], which entailed cables fabricated with different cabling machines. However, one can observe good consistency among cables made with similar strands.

As can be seen, the new PIT design (PIT2) has dramatically improved its performance reducing I_c degradation to the level observed in MJR strands. The effect appears to depend on PF only, not on the geometry of the cable (i.e. there is no observable difference between rectangular and keystone cables having the same PF). For all technologies, the effective J_c has an almost flat behaviour over the whole PF range. Except in the case of ITER (and the old generation of PIT), the effective J_c is always larger than for a hypothetical uncompacted cable with round strands. However, a moderate PF of 88–90% was chosen for the R&D dipole models to avoid excessively sharp edges.

4.2. Simulation of cabling degradation

In order to simulate the cabling process, Nb_3Sn strands of different technologies were rolled down to various sizes, heat treated and tested. The cross-section of the rolled strand is shown in figure 5, where t is the strand thickness and w its width after rolling. Strand deformation was characterized by strain, defined by $(d - t)/d$, where d is the original round strand diameter before rolling.

The critical current of the rolled strands was then compared at 4.2 K and 12 T with that of the same strand extracted from cables with various packing factors. The results are shown in figures 6 and 7 for the old PIT design (PIT1) and for the MJR. By matching at best the data points for the rolled and extracted strands, one can find a range of strain for rolled strands where a reasonably good correlation of I_c degradation

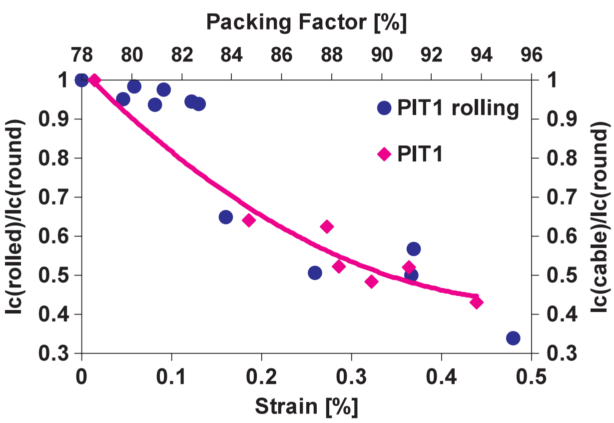

Figure 6. Effect on the I_c of rolling versus cabling for the old PIT (PIT1) strand at 4.2 K and 12 T.

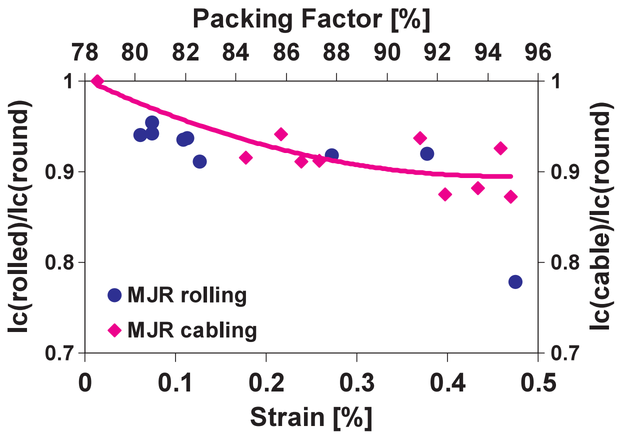

Figure 7. Effect on the I_c of rolling versus cabling for the MJR strand at 4.2 K and 12 T.

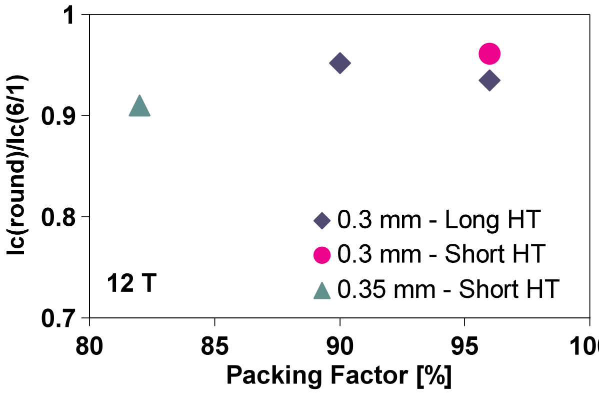

Figure 8. Normalized I_c at 4.2 K and 12 T of the extracted sub-strands as a function of the 6/1 strand assembly PF.

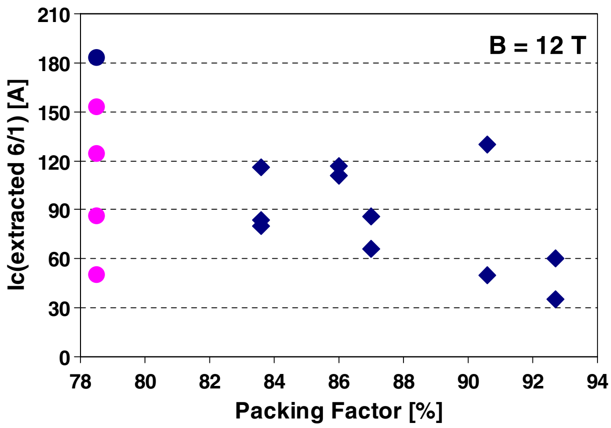

Figure 9. Strand I_c at 4.2 K and 12 T of 6/1 strand assemblies extracted from Rutherford cables versus cable PF (lozenges), compared with those of a 6/1 assembly after cutting single sub-strands one by one (dots).

is observed between the latter and extracted strands. Therefore, it appears that rolling down strands is an excellent method to simulate the effect of I_c degradation due to cabling, and can therefore be used instead of it.

4.3. Studies of two-stage cable

Studies of the cabling degradation of two-stage cables were performed on cables with 6 around 1 (6/1) multiple strands (see figure 1, bottom). This was done in two steps. First, single sub-strands of 0.35 mm were extracted from a 6/1 strand assembly and heat treated together with round sub-strands. The normalized I_c at 4.2 K and 12 T of the extracted sub-strands is shown in figure 8 as a function of the strand assembly PF. After this first stage, degradation is $<10\%$ and could probably be further reduced. Then, following fabrication of a Rutherford cable made of 28-strand assemblies, 6/1 strand assemblies of 1 mm were extracted from the cable and heat treated with round 6/1 strands. Figure 9 shows I_c measurements at 4.2 K and 12 T of the round 6/1 strand (dark dot at PF $= 78.5\%$), and of the 6/1 strands extracted from the Rutherford cable in the rest of the PF range (dark lozenges).

To check whether the large degradation and large spread in the data could be due to micro-fractures of the sub-strands, a sub-strand of the round 6/1 assembly was cut and the 5/1 assembly tested again, then another sub-strand was cut and the 4/1 assembly tested again, and so on. These latter data, which are also shown in figure 9 (grey dots), seem to confirm such a hypothesis. The I_c values of the extracted strands lie in the vicinity of the discrete I_c values of the $n/1$ assemblies. Also, the I_c difference between results obtained for extracted strands with the same PF is about the same or a multiple of the current carried by single sub-strands, which is about 30 A. This value confirms that in an $n/1$ assembly, the current is shared among the outer sub-strands only, with the central one carrying a negligible fraction.

5. Summary

Superconducting strands and cables are substantial in magnet R&D in that they determine magnet performance and cost. Dozens of Rutherford cables of a variety of Nb_3Sn strand technologies were used in these cabling degradation studies, which represent the largest systematic data set so far on the topic. A method was developed to simulate cabling and the strains applied during the process. This method can be used instead to evaluate cabling degradation. Making two-stage cables in-house will allow searching the minimum strand size that withstands such a procedure.

Acknowledgments

The authors thank Tom Wokas and Tom Van Raes whose help was substantial for the success of the Strand & Cable R&D at Fermilab.

References

[1] Andreev N *et al* 2002 Development and test of single-bore cos-theta Nb_3Sn dipole models with cold iron yoke *IEEE Trans. Appl. Supercond.* **12** 332
[2] Novitski I *et al* 2001 Design and mechanical analysis of a single-layer common coil dipole for VLHC *IEEE Trans. Appl. Supercond.* **11** 2276
[3] Barzi E *et al* 2004 Sensitivity of Nb_3Sn Rutherford-type cables to transverse pressure *Supercond. Sci. Technol.* **17**
[4] Barzi E *et al* 2001 Study of Nb_3Sn strands for Fermilab's high field dipole models *IEEE Trans. Appl. Supercond.* **11** 3595
[5] Barzi E *et al* 1999 Study of strand critical current degradation in a Rutherford-type Nb_3Sn cable *CEC/ICMC'99 (Montreal, Canada, July 1999)* vol 46B pp 1091–2000
[6] Barzi E *et al* 2001 Strand critical current degradation in Nb_3Sn Rutherford cables *IEEE Trans. Appl. Supercond.* **11** 2134